



# Joint relative position and velocity estimation for an anchorless network of mobile nodes<sup>☆</sup>



Raj Thilak Rajan<sup>a,b,\*</sup>, Geert Leus<sup>b</sup>, Alle-Jan van der Veen<sup>b</sup>

<sup>a</sup> Netherlands Institute for Radio Astronomy (ASTRON), Oude Hoogeveensedijk 4, Dwingeloo, The Netherlands

<sup>b</sup> TU Delft, Fac. EEMCS, Mekelweg 4, 2628 CD Delft, The Netherlands

## ARTICLE INFO

### Article history:

Received 18 September 2014

Received in revised form

23 December 2014

Accepted 27 February 2015

Available online 18 March 2015

### Keywords:

Dynamic ranging

Relative kinematics

Multi-dimensional scaling (MDS)

Anchor-free wireless network

Cramér Rao bounds

## ABSTRACT

Localization is a fundamental challenge for any network of nodes, in particular when the nodes are in motion and no reference nodes are available. Traditionally, the Multi-dimensional scaling (MDS) algorithm is employed at discrete time instances using pairwise distance measurements to find the relative node positions (with arbitrary rotation). In this paper, we present a novel framework to localize an *anchorless network of mobile nodes* given only time-varying inter-nodal distances. The time derivatives of the pairwise distances are used to jointly estimate the initial relative position and relative velocity of the nodes. Under linear velocity assumption for a small time duration, we show that the combination of the initial relative positions and relative velocity beget the relative motion of the nodes at discrete time instances. The proposed approach can be seen as an extension of the classical MDS, wherein Doppler measurements, if available, can be readily incorporated. We derive Cramér Rao bounds and perform simulations to evaluate the performance of the proposed estimators. Furthermore, the computational complexity and the benefits of the proposed algorithms are also presented.

© 2015 Elsevier B.V. All rights reserved.

## 1. Introduction

Localization is a key requirement for the deployment of wireless networks in a wide range of applications. There are numerous absolute localization algorithms, such as Time of Arrival (ToA), Time Difference of Arrival (TDoA) and Received Signal Strength (RSS) which cater to anchored networks, where a few node positions are known [2]. Alternatively, when there are no reference anchors, then the relative positions of the nodes, up to a rotation and translation, can still be obtained using Multi-Dimensional Scaling (MDS) based

solutions [3,4]. Such anchorless networks arise naturally when the nodes are deployed in inaccessible locations or when anchor information is known intermittently. In both anchored or anchorless scenarios, pairwise distances are one of the key inputs for almost all localization techniques. For stationary nodes, these pairwise distances are classically obtained by measuring the propagation delays of multiple time stamp exchanges between the nodes and averaging these measurements over a time period.

A step further, when the nodes are mobile, then conventionally either the nodes are considered relatively stationary within desired accuracies for the complete duration of the measurement interval (i.e., multiple distance measurements) [5] or Doppler measurements are utilized [6]. Unfortunately, Doppler measurements are not always available and the assumption on the node positional stability for large time periods is simply unpractical in many applications. For a mobile network, the application of classical MDS-based

<sup>☆</sup> This research was funded in part by the STW OLFAR project (Contract Number: 10556) within the ASSYS perspectief program. A part of this work has been published in IEEE CAMSAP 2013 conference [1].

\* Corresponding author at: Netherlands Institute for Radio Astronomy (ASTRON), Oude Hoogeveensedijk 4, Dwingeloo, The Netherlands.

E-mail address: [rajan@astron.nl](mailto:rajan@astron.nl) (R.T. Rajan).

relative positioning at every time instant yields a sequence of position matrices with arbitrary rotation, thereby providing no information on the relative velocities of the nodes. We define the term *relative velocities* as the velocity vectors of the nodes, up to a common rotation, translation and reflection. This has, to the best of the authors' knowledge, not yet been investigated in the literature. Given the relative velocities up to the appropriate rotation, the time-varying positions can be readily obtained for a linear mobility model. Hence, the estimation of relative velocities therefore constitutes a paramount challenge to be solved in next-generation localization technologies.

### 1.1. Applications

Our motivation for this work is triggered by *inaccessible mobile wireless networks*, which have partial or no information of absolute coordinates and/or clock references. Such scenarios are prevalent in under-water communications [7], indoor positioning systems [8], autonomous swarm networks [9] and envisioned space based satellite networks with minimal ground segment capability. A particular project of interest is Orbiting Low Frequency Antennas for Radio astronomy (OLFAR) [10], a Dutch funded program which aims to design and develop a detailed system concept for a scalable interferometric array of more than 10 identical, autonomous satellites in space (far from earth) to be used as a scientific instrument for ultra long wavelength observations (0.3 kHz to 30 MHz). Due to limitations of earth-based tracking, the OLFAR cluster will be an independent cooperative network of nodes, whose positions and velocities need to be estimated jointly.

### 1.2. Contributions

In this paper, our quest is to localize an *anchorless network of mobile nodes*, given time-varying pairwise distance measurements. We propose a two-step approach to solve this problem. Firstly, we approximate the time-varying pairwise propagation delays (and subsequently the distances) between the mobile nodes as a Taylor series in time, which is aptly termed Dynamic Ranging (Section 2). A simple yet efficient time-basis is employed to estimate the derivatives of the pairwise distances at a given time instant (Section 3). Secondly, under the assumption of constant velocity for a short time duration, we show that the relative position of each node is dependent only on the initial relative position, the relative velocity and a unique rotation matrix (Section 4) [1]. Furthermore, we also show that the solutions to the unknown initial relative position, the relative velocity and the rotation matrix lie in the first three derivatives of the time-varying pairwise distance. Subsequently, we present MDS-like and least squares solutions to estimate the unknown parameters in Section 5 and Cramér Rao Bounds are derived in Section 5.3. Finally, based on the proposed estimators we propose two algorithms, namely LMDS and CMDS to estimate the relative positions of the nodes over discrete time intervals (Section 6). Simulations are conducted to evaluate the performance of the proposed estimators in Section 7. The novelty of our work lies in the proposed framework and subsequent

estimators to estimate time-varying relative motion in Euclidean space.

*Notation:* The element wise matrix Hadamard product is denoted by  $\odot$ . We denote the element-wise matrix exponent as  $(\cdot)^{\odot N}$  and  $\oslash$  indicates the element-wise Hadamard division. The Kronecker product is indicated by  $\otimes$ , the transpose operator by  $(\cdot)^T$  and the pseudo-inverse by  $(\cdot)^\dagger$ . The vectors of ones and zeros are given by  $\mathbf{1}_N = [1, 1, \dots, 1]^T$ ,  $\mathbf{0}_N = [0, 0, \dots, 0]^T \in \mathbb{R}^{N \times 1}$ , respectively. The Euclidean norm is denoted by  $\|\cdot\|$ ,  $\mathbf{I}_N$  is a  $N \times N$  identity matrix and  $\mathbf{0}_{M,N}$  is a  $M \times N$  matrix of zeros. A diagonal matrix of the vector  $\mathbf{a}$  is represented by  $\text{diag}(\mathbf{a})$  and a block diagonal matrix  $\mathbf{A} = \text{bdiag}(\mathbf{A}_1, \mathbf{A}_2, \dots, \mathbf{A}_N)$  consists of matrices  $\mathbf{A}_1, \mathbf{A}_2, \dots, \mathbf{A}_N$  along the diagonal and 0 elsewhere.  $\text{vec}(\mathbf{A})$  operator reshapes the matrix  $\mathbf{A}$  into a vector.  $a \sim \mathcal{N}(\mu, \Sigma)$  is shorthand for a randomly distributed Gaussian variable with mean  $\mu$  and variance  $\Sigma$ .

## 2. Dynamic ranging

### 2.1. Range model

Consider a cluster of  $N$  nodes in a  $P$ -dimensional Euclidean space. If the nodes are fixed, then the pairwise propagation delay at time  $t_0$  between a given node pair  $(i, j)$  is defined as

$$\tau_{ij}(t_0) \equiv \tau_{ji}(t_0) \triangleq c^{-1} d_{ij}(t_0), \quad (1)$$

where  $d_{ij}(t_0)$  is the fixed distance between the node pair at  $t_0$  and  $c$  is the speed of the electromagnetic wave in the medium. However, when the nodes are mobile, the relative distances between the nodes are a non-linear function of time (for  $P \geq 2$ ), even when the nodes are in linear motion. For a small time interval  $\Delta t_k = t_k - t_0$ , we consider these relative distances as a smoothly varying polynomial in time. The propagation delay  $\tau_{ij}(t_k) \equiv \tau_{ji}(t_k)$  between a given node pair  $(i, j)$  can be expanded classically as an infinite Taylor series around a time instant  $t_0$  within the neighborhood  $\Delta t_k$ . As an extension of the second-order distance model [11], we have

$$\tau_{ij}(t_0 + \Delta t_k) \triangleq c^{-1} d_{ij}(t_0 + \Delta t_k) \triangleq c^{-1} d_{ij}(t_k), \quad (2)$$

where  $d_{ij}(t_k)$  is the distance at  $t_k = t_0 + \Delta t_k$ , given by

$$d_{ij}(t_k) \simeq r_{ij} + \frac{\dot{r}_{ij}}{1!} \Delta t_k + \frac{\ddot{r}_{ij}}{2!} \Delta t_k^2 + \dots, \quad (3)$$

where  $[r_{ij}, \dot{r}_{ij}, \ddot{r}_{ij}, \dots]^T \in \mathbb{R}^{L \times 1}$  are the range parameters for the  $L$ th order approximation of the time-varying distance. The first coefficient  $r_{ij} \equiv d_{ij}(t_0)$  is the initial pairwise distance and the following  $L-1$  coefficients are successive derivatives of  $r_{ij}$  at  $t_0$ . Without loss of generality, assuming  $t_0 = 0$ , we have  $t_k = \Delta t_k$  and subsequently (2) and (3) simplify to the Maclaurin series as

$$\tau_{ij}(t_k) = c^{-1} \left( r_{ij} + \dot{r}_{ij} t_k + \frac{\ddot{r}_{ij}}{2!} t_k^2 + \dots \right). \quad (4)$$

The polynomial range basis is simplified further by introducing

$$[\underline{r}_{ij}, \underline{\dot{r}}_{ij}, \underline{\ddot{r}}_{ij}, \dots]^T \triangleq \text{diag}(\mathbf{f})^{-1} [r_{ij}, \dot{r}_{ij}, \ddot{r}_{ij}, \dots]^T, \quad (5)$$

where  $\mathbf{f} = c[1, 1!, 2!, \dots]^T \in \mathbb{R}^{L \times 1}$ , such that (4) is

$$\tau_{ij}(t_k) \triangleq c^{-1} d_{ij}(t_k) = r_{ij} + \dot{r}_{ij} t_k + \ddot{r}_{ij} t_k^2 + \dots \quad (6)$$

Now, for the entire network of  $N$  nodes, the *unique* pairwise ranges are collected in a vector  $\mathbf{r} \in \mathbb{R}^{\bar{N} \times 1}$ , where  $\bar{N} = \binom{N}{2}$  is the number of unique pairwise baselines. Along similar lines, we define  $\dot{\mathbf{r}} \in \mathbb{R}^{\bar{N} \times 1}$ ,  $\ddot{\mathbf{r}} \in \mathbb{R}^{\bar{N} \times 1}$  and corresponding higher-order terms. The unknown range parameters for all pairwise links are collected under the vector  $\boldsymbol{\theta} = [\mathbf{r}^T, \dot{\mathbf{r}}^T, \ddot{\mathbf{r}}^T, \dots]^T \in \mathbb{R}^{\bar{N}L \times 1}$ . Furthermore, similar to the definition of  $\boldsymbol{\theta}$ , we define  $\underline{\boldsymbol{\theta}} = [\underline{\mathbf{r}}^T, \underline{\dot{\mathbf{r}}}^T, \underline{\ddot{\mathbf{r}}}^T, \dots]^T \in \mathbb{R}^{\bar{N}L \times 1}$ , where  $\underline{\mathbf{r}} \in \mathbb{R}^{\bar{N} \times 1}$ ,  $\underline{\dot{\mathbf{r}}} \in \mathbb{R}^{\bar{N} \times 1}$ ,  $\underline{\ddot{\mathbf{r}}} \in \mathbb{R}^{\bar{N} \times 1}$  and corresponding higher-order terms are *modified* range parameters. The relationship between  $\boldsymbol{\theta}$  and  $\underline{\boldsymbol{\theta}}$ , using (5), is then

$$\boldsymbol{\theta} = (\text{diag}(\mathbf{f}) \otimes \mathbf{I}_{\bar{N}}) \underline{\boldsymbol{\theta}} \quad (7)$$

**Remark 1 (Doppler measurements).** Observe that in essence,  $\mathbf{r}$  is the Time of Arrival (ToA) at  $t_0$ , the range rate  $\dot{\mathbf{r}}$  is the radial velocity (as obtained from a Doppler shift) and the second order range parameter  $\ddot{\mathbf{r}}$  is the rate of radial velocity (as observed from a Doppler spread) between the nodes at  $t = t_0$ . These range coefficients can be readily incorporated if these measurements are available.

## 2.2. Data model

We now consider a relaxed Two-Way Ranging (TWR) setup for collecting distance information as follows. Let each node pair ( $ij$ ) within the network be capable of communicating with each other as shown in Fig. 1. The nodes communicate  $K$  messages back and forth, and the time of transmission and reception is registered independently at the respective nodes. The  $k$ th time stamp recorded at node  $i$  when communicating with node  $j$  is denoted by  $T_{ij,k}$  and similarly at node  $j$  the time stamp is  $T_{ji,k}$ . The direction of the communication is indicated by  $E_{ij,k}$ , where  $E_{ij,k} = +1$  for transmission from node  $i$  to node  $j$  and  $E_{ij,k} = -1$  for transmission from node  $j$  to node  $i$ . Under ideal noiseless conditions, the propagation delay between the node pair at the  $k$ th time instant is  $\tau_{ij,k} \triangleq E_{ij,k}(T_{ji,k} - T_{ij,k})$ , and in conjunction with the polynomial approximation (6),

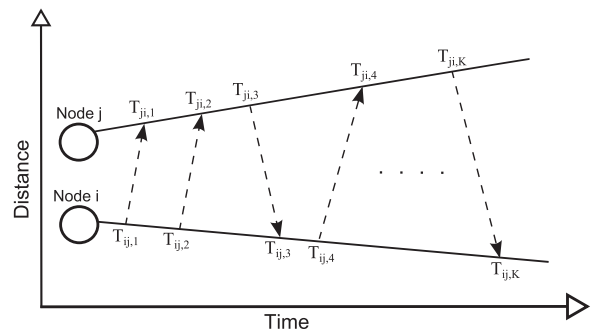


**Fig. 1.** Pair of mobile nodes: a generalized Two-Way Ranging (TWR) between a pair of mobile nodes, where the solid-skewed lines indicate the linear motion of the nodes. During the linear motion, the nodes transmit and receive  $K$  time stamps are recorded at the respective nodes. Similar to [5,11,12], we levy no constraints on the sequence, direction or number of communications.

we have

$$\tau_{ij,k} \triangleq E_{ij,k}(T_{ji,k} - T_{ij,k}) = r_{ij} + \dot{r}_{ij} T_{ij,k} + \ddot{r}_{ij} T_{ij,k}^2 + \dots, \quad (8)$$

where without loss of generality we have replaced  $t_k$  with  $T_{ij,k}$ .

**Remark 2 (Synchronized nodes).** By replacing *true* time  $t_k$  by  $T_{ij,k}$ , we assume without loss of generality that  $T_{ij,k}$  is in the neighborhood of  $t_0 = 0$  and the propagation delay is measured as a function of the local time at node  $i$ . Furthermore, we also assume that the clocks of these nodes are synchronized. This is a valid assumption since for an asynchronous network of mobile nodes, the clock parameters (up to first order) can be decoupled from the range parameters and the distances can be estimated efficiently as shown in [5,11,12].

In practice, the time measurements are also corrupted with noise and hence (8) is

$$\begin{aligned} r_{ij} + \dot{r}_{ij}(T_{ij,k} + q_{i,k}) + \ddot{r}_{ij}(T_{ij,k} + q_{i,k})^2 + \dots \\ = E_{ij,k} \left( (T_{ji,k} + q_{j,k}) - (T_{ij,k} + q_{i,k}) \right), \end{aligned} \quad (9)$$

where  $q_{i,k} \sim \mathcal{N}(0, \Sigma_i)$  and  $q_{j,k} \sim \mathcal{N}(0, \Sigma_j)$  are modelled as Gaussian i.i.d. noise variables, plaguing the timing measurements at node  $i$  and node  $j$ , respectively. Rearranging the terms, we have

$$r_{ij} + \dot{r}_{ij} T_{ij,k} + \ddot{r}_{ij} T_{ij,k}^2 + \dots = E_{ij,k}(T_{ji,k} - T_{ij,k}) + q_{ij,k}, \quad (10)$$

where

$$q_{ij,k} = E_{ij,k}(q_{j,k} - q_{i,k}) - (\dot{r}_{ij} q_{i,k} + 2\ddot{r}_{ij} T_{ij,k} q_{i,k} + \ddot{r}_{ij} q_{i,k}^2 + \dots). \quad (11)$$

For wireless communication with  $c = 3 \times 10^8$  m/s, note that the modified range parameters are scaled by  $c^{-1}$  (7). Furthermore, since the dynamic range model is proposed for a small time interval, the term  $(\dot{r}_{ij} q_{i,k} + 2\ddot{r}_{ij} T_{ij,k} q_{i,k} + \ddot{r}_{ij} q_{i,k}^2 + \dots)$  is relatively small and subsequently the noise vector plaguing the measurements can be approximated as  $q_{ij,k} \approx E_{ij,k}(q_{j,k} - q_{i,k})$  which begets

$$q_{ij,k} \sim \mathcal{N}(0, \Sigma_{ij}), \quad (12)$$

where  $\Sigma_{ij} = \Sigma_i + \Sigma_j$ . Aggregating all  $K$  packets, we have

$$\underbrace{\begin{bmatrix} \mathbf{1}_K & \mathbf{t}_{ij} & \mathbf{t}_{ij}^{\odot 2} & \dots \end{bmatrix}}_{\mathbf{A}_{ij}} \underbrace{\begin{bmatrix} r_{ij} \\ \dot{r}_{ij} \\ \ddot{r}_{ij} \\ \vdots \end{bmatrix}}_{\boldsymbol{\theta}_{ij}} = \boldsymbol{\tau}_{ij} + \mathbf{q}_{ij}, \quad (13)$$

where

$$\boldsymbol{\tau}_{ij} \triangleq \mathbf{e}_{ij} \odot (\mathbf{t}_{ji} - \mathbf{t}_{ij}) \in \mathbb{R}^{K \times 1}, \quad (14)$$

$$\mathbf{e}_{ij} = [E_{ij,1}, E_{ij,2}, \dots, E_{ij,K}]^T \in \mathbb{R}^{K \times 1}, \quad (15)$$

$$\mathbf{t}_{ij} = [T_{ij,1}, T_{ij,2}, \dots, T_{ij,K}]^T \in \mathbb{R}^{K \times 1}. \quad (16)$$

The known Vandermonde matrix  $\mathbf{A}_{ij} \in \mathbb{R}^{K \times L}$  contains the measured time stamps and is full column rank if  $T_{ij,k}$  are unique. The direction vector  $\mathbf{e}_{ij}$  is encapsulated in the propagation delay  $\boldsymbol{\tau}_{ij}$  and  $\boldsymbol{\theta}_{ij} \in \mathbb{R}^{L \times 1}$  is a vector containing the unknown range parameters. The noise vector on this linear system is  $\mathbf{q}_{ij} = [q_{ij,1}, q_{ij,2}, \dots, q_{ij,K}]^T \in \mathbb{R}^{K \times 1}$ , where  $q_{ij,k}$  is given by (12) and the corresponding covariance matrix is

$$\boldsymbol{\Sigma}_{ij} \triangleq \mathbb{E}[\mathbf{q}_{ij} \mathbf{q}_{ij}^T] = \boldsymbol{\Sigma}_{ij} \mathbf{1}_K \in \mathbb{R}^{K \times K}. \quad (17)$$

For a network of  $N$  nodes, the normal equation (13) can be extended to the *Dynamic Ranging* model:

$$\underbrace{[\mathbf{I}_N \otimes \mathbf{1}_K \quad \mathbf{T} \quad \mathbf{T}^{\odot 2} \quad \dots]}_{\mathbf{A}} \underbrace{\begin{bmatrix} r \\ \dot{r} \\ \ddot{r} \\ \vdots \end{bmatrix}}_{\boldsymbol{\theta}} = \boldsymbol{\tau} + \mathbf{q}, \quad (18)$$

where

$$\mathbf{T} = \text{bdiag}(\mathbf{t}_{12}, \mathbf{t}_{13}, \dots, \mathbf{t}_{1N}, \mathbf{t}_{23}, \dots) \in \mathbb{R}^{\bar{N}K \times \bar{N}}, \quad (19)$$

$$\boldsymbol{\tau} = [\boldsymbol{\tau}_{12}^T, \boldsymbol{\tau}_{13}^T, \dots, \boldsymbol{\tau}_{1N}^T, \boldsymbol{\tau}_{23}^T, \dots]^T \in \mathbb{R}^{\bar{N}K \times 1}, \quad (20)$$

contain the time stamp exchanges of the  $\bar{N}$  unique pairwise links in the network and  $\boldsymbol{\theta} \in \mathbb{R}^{\bar{N}L \times 1}$  contains the unknown range parameters for the entire network. The noise vector is  $\mathbf{q} = [\mathbf{q}_{12}^T, \mathbf{q}_{13}^T, \dots, \mathbf{q}_{1N}^T, \mathbf{q}_{23}^T, \dots]^T \in \mathbb{R}^{\bar{N}K \times 1}$  and the covariance matrix is

$$\boldsymbol{\Sigma} \triangleq \mathbb{E}[\mathbf{q}\mathbf{q}^T] \in \mathbb{R}^{\bar{N}K \times \bar{N}K}. \quad (21)$$

**Remark 3** (*Mobility of the nodes*). In (8), we implicitly assumed that the nodes are relatively fixed during a time period of  $\Delta t_k = |T_{ij,k} - T_{ji,k}|$  i.e., the propagation time of the message. This is a much weaker assumption compared to traditional TWR, where for a pair of fixed nodes (i.e.,  $L=1$ ), the pairwise distance is assumed to be invariant for the total measurement period  $\Delta t = |T_{ij,K} - T_{ij,1}|$ . In reality, when the nodes are mobile, the distance at each  $k$ th time instant is dissimilar and this feature is naturally incorporated in the presented Dynamic Ranging model.

### 3. Dynamic ranging algorithm

Suppose that we have collected all the TWR timing data in  $\mathbf{A}$  and  $\boldsymbol{\tau}$ , then in this section we find an estimate for the unknown  $\boldsymbol{\theta}$  using the model (18). Given an estimate of  $\boldsymbol{\theta}$ , the range coefficients  $\boldsymbol{\theta} = [\mathbf{r}^T, \dot{\mathbf{r}}^T, \ddot{\mathbf{r}}^T, \dots]^T$  can be directly obtained from (7).

#### 3.1. Weighted least squares

Under the assumption that the covariance matrix  $\boldsymbol{\Sigma}$  is known, a Weighted Least Squares (WLS) solution  $\hat{\boldsymbol{\theta}}$  is obtained by minimizing the  $l_2$  norm of the linear system (18), leading to

$$\hat{\boldsymbol{\theta}} = \arg \min_{\boldsymbol{\theta}} \|\boldsymbol{\Sigma}^{-1/2}(\mathbf{A}\boldsymbol{\theta} - \boldsymbol{\tau})\|^2 \quad (22)$$

$$= (\mathbf{A}^T \boldsymbol{\Sigma}^{-1} \mathbf{A})^{-1} \mathbf{A}^T \boldsymbol{\Sigma}^{-1} \boldsymbol{\tau}, \quad (23)$$

which is a valid solution if  $K \geq L$  for each of the  $\bar{N}$  pairwise links. More generally, when the polynomial model order  $L$  is unknown in (3), order recursive least squares algorithms (such as iMGLS [12]) can be employed to obtain the range coefficients for increasing values of  $L$ , until an optimal polynomial fit for (22) is reached.

#### 3.2. Distributed weighted least squares

If we consider independent pairwise communication between all the nodes, with no broadcasting, then the noise in each pairwise link is independent of each other and subsequently the covariance matrix (21) simplifies to

$$\boldsymbol{\Sigma} = \text{bdiag}(\boldsymbol{\Sigma}_{12}, \boldsymbol{\Sigma}_{13}, \dots, \boldsymbol{\Sigma}_{1N}, \boldsymbol{\Sigma}_{23}, \dots). \quad (24)$$

In which case, the centralized system (18) is a cascade of pairwise linear systems (13) and subsequently (23) is a generalized version of solving the distributed pairwise system for estimating the pairwise range parameters  $\boldsymbol{\theta}_{ij}$  independently as

$$\begin{aligned} \hat{\boldsymbol{\theta}}_{ij} &= \arg \min_{\boldsymbol{\theta}_{ij}} \|\boldsymbol{\Sigma}_{ij}^{-1/2}(\mathbf{A}_{ij}\boldsymbol{\theta}_{ij} - \boldsymbol{\tau}_{ij})\|^2 \\ &= (\mathbf{A}_{ij}^T \boldsymbol{\Sigma}_{ij}^{-1} \mathbf{A}_{ij})^{-1} \mathbf{A}_{ij}^T \boldsymbol{\Sigma}_{ij}^{-1} \boldsymbol{\tau}_{ij}, \end{aligned} \quad (25)$$

which, similar to (23), has a valid solution for  $K \geq L$  for each pairwise link. It is worth noting that when the noise is correlated between pairwise links, the distributed weighted least squares (25) may be sub-optimal. In this case, a consensus based distributed least squares algorithm [13] can be employed for improved solutions.

#### 3.3. Cramér Rao bounds

The Cramér Rao lower Bound (CRB) [14] for the linear model (18) is

$$\boldsymbol{\Sigma}_{\boldsymbol{\theta}} = (\mathbf{A}^T \boldsymbol{\Sigma}^{-1} \mathbf{A})^{-1}, \quad (26)$$

and in combination with the range scaling (7), the CRB on  $\boldsymbol{\theta}$  is given by

$$\boldsymbol{\Sigma}_{\boldsymbol{\theta}} = (\text{diag}(\mathbf{f}) \otimes \mathbf{I}_{\bar{N}})(\mathbf{A}^T \boldsymbol{\Sigma}^{-1} \mathbf{A})^{-1}(\text{diag}(\mathbf{f}) \otimes \mathbf{I}_{\bar{N}}), \quad (27)$$

where

$$\boldsymbol{\Sigma}_{\boldsymbol{\theta}} = \begin{bmatrix} \boldsymbol{\Sigma}_r & * & * & * \\ * & \boldsymbol{\Sigma}_{\dot{r}} & * & * \\ * & * & \boldsymbol{\Sigma}_{\ddot{r}} & * \\ * & * & * & \ddots \end{bmatrix}, \quad (28)$$

is the lowest variance attained by any unbiased estimate of the range parameters  $\boldsymbol{\theta} = [\mathbf{r}^T, \dot{\mathbf{r}}^T, \ddot{\mathbf{r}}^T, \dots]^T$ . It is worth noting that (23) achieves these lower bounds for an appropriate  $L$ .

**Remark 4** (*Direction independence*). In general, observe that the proposed solution (23) is feasible for any direction marker  $E_{ij,k}$ , which is incorporated in  $\boldsymbol{\tau}$  (14). In addition, the lower bounds are unaffected by the choice of direction vector  $\mathbf{e}_{ij}$ ,  $\forall i, j \leq N$ , since all direction vectors are encapsulated in the measurement vector  $\boldsymbol{\tau}_{ij}$ , which is not a part of the CRB (27). Hence communication between the nodes could be arbitrary or one way, and need not be necessarily bi-directional. However, this is not true for an asynchronous network, where two-way communication is pivotal in jointly estimating the clock and range parameters [12]. In addition, we impose no pre-requisite on the number, sequence or direction of the communication links [5,12]. Therefore, the proposed solution is amenable to prevalent Two Way Ranging (TWR) protocols, such as classical

pairwise communication [15], passive listening and broadcasting [16].

#### 4. Relative kinematics

In the previous section, we estimated  $\hat{\mathbf{Q}}$  which contains the solution to the unknown range derivatives  $\hat{\boldsymbol{\theta}} = [\hat{\mathbf{r}}^T, \hat{\dot{\mathbf{r}}}^T, \hat{\ddot{\mathbf{r}}}^T, \dots]$ . Our next motive is to use these range derivatives to estimate the positions of the mobile nodes. When the nodes are in motion, similar to the pairwise range rates, the position vector of each node is also a Taylor series in time. However, exploiting piecewise linearity, we assume that the nodes are in linear motion with no acceleration, which is valid for a sufficiently small measurement period. Note that despite this assumption, the pairwise distance is still non-linear.

##### 4.1. Absolute linear motion

Let the position of  $N$  ( $N \geq P$ ) nodes in a  $P$ -dimensional Euclidean space at the  $k$ th time instant be given by  $\mathbf{X}_k = [\mathbf{x}_{1,k}, \mathbf{x}_{2,k}, \dots, \mathbf{x}_{N,k}] \in \mathbb{R}^{P \times N}$ , where  $\mathbf{x}_{i,k} \in \mathbb{R}^{P \times 1}$  is the position vector of the  $i$ th node at the  $k$ th message exchange. Furthermore, the  $i$ th node has velocity  $\mathbf{y}_i \in \mathbb{R}^{P \times 1}$  and all such velocities are collected in  $\mathbf{Y} = [\mathbf{y}_1, \mathbf{y}_2, \dots, \mathbf{y}_N] \in \mathbb{R}^{P \times N}$ . Then, under a linear motion assumption, we have

$$\frac{d\mathbf{y}_i}{dt} = \mathbf{0}_P \quad \forall i \leq N. \quad (29)$$

Now, let  $\Delta t_k = t_k - t_0$  where for the sake of notational convenience and without loss of generality, we assume  $t_k = T_{ij,k} \forall k$ , then the position matrix at the  $k$ th time instant is

$$\mathbf{X}_k = \mathbf{X} + \Delta t_k \mathbf{Y}, \quad (30)$$

where  $\mathbf{X} \triangleq \mathbf{X}_0 = [\mathbf{x}_1, \mathbf{x}_2, \dots, \mathbf{x}_N]$  is the initial position matrix at time instant  $t_0$  and  $\mathbf{X}_k$  only depends on the initial Position and Velocity (PV) of the nodes.

##### 4.2. Range derivatives

To estimate the position matrix  $\mathbf{X}_k$ , we begin by stating explicit expressions for the range derivatives  $[\mathbf{r}, \dot{\mathbf{r}}, \ddot{\mathbf{r}}, \dots]$  in terms of  $\mathbf{X}, \mathbf{Y}$  under linear velocity assumption. The pairwise distance  $d_{ij}(t)$  between a node pair  $(i, j)$  in  $P \geq 2$  dimensional Euclidean space is a non-linear function of time, even if the nodes are only in linear motion. As derived in Appendix A, the range parameters  $[r_{ij}, \dot{r}_{ij}, \ddot{r}_{ij}, \dots]$  at  $t = t_0$  satisfy

$$r_{ij} = \sqrt{\mathbf{x}_i^T \mathbf{x}_i + \mathbf{x}_j^T \mathbf{x}_j - 2\mathbf{x}_i^T \mathbf{x}_j}, \quad (31a)$$

$$\dot{r}_{ij} = r_{ij}^{-1} (\mathbf{x}_i - \mathbf{x}_j)^T (\mathbf{y}_i - \mathbf{y}_j), \quad (31b)$$

$$\ddot{r}_{ij} = r_{ij}^{-1} (\|\mathbf{y}_i - \mathbf{y}_j\|^2 - \dot{r}_{ij}^2). \quad (31c)$$

Although these range parameters can be estimated up to the  $(L-1)$ th order efficiently (as demonstrated in Section 3), in the rest of this paper we utilize the information only up to  $L=3$  for estimating the relative PV. Rearranging the equations for  $r_{ij}, \dot{r}_{ij}, \ddot{r}_{ij}$ , from (31) we

obtain

$$r_{ij}^2 = (\mathbf{x}_i - \mathbf{x}_j)^T (\mathbf{x}_i - \mathbf{x}_j), \quad (32a)$$

$$r_{ij} \dot{r}_{ij} = (\mathbf{x}_i - \mathbf{x}_j)^T (\mathbf{y}_i - \mathbf{y}_j), \quad (32b)$$

$$r_{ij} \ddot{r}_{ij} + \dot{r}_{ij}^2 = (\mathbf{y}_i - \mathbf{y}_j)^T (\mathbf{y}_i - \mathbf{y}_j). \quad (32c)$$

Extending the above equations for all  $N$  nodes, defining  $\mathbf{g}_{xx} = \text{diag}(\mathbf{X}^T \mathbf{X}) \in \mathbb{R}^{N \times 1}$ ,  $\mathbf{g}_{xy} = \text{diag}(\mathbf{X}^T \mathbf{Y}) \in \mathbb{R}^{N \times 1}$  and  $\mathbf{g}_{yy} = \text{diag}(\mathbf{Y}^T \mathbf{Y}) \in \mathbb{R}^{N \times 1}$ , we have

$$\mathbf{R}^{\circ 2} = \mathbf{g}_{xx} \mathbf{1}_N^T + \mathbf{1}_N \mathbf{g}_{xx}^T - 2\mathbf{X}^T \mathbf{X}, \quad (33a)$$

$$\mathbf{R} \circ \dot{\mathbf{R}} = \mathbf{g}_{xy} \mathbf{1}_N^T + \mathbf{1}_N \mathbf{g}_{xy}^T - \mathbf{X}^T \mathbf{Y} - \mathbf{Y}^T \mathbf{X}, \quad (33b)$$

$$\mathbf{R} \circ \ddot{\mathbf{R}} + \dot{\mathbf{R}}^{\circ 2} = \mathbf{g}_{yy} \mathbf{1}_N^T + \mathbf{1}_N \mathbf{g}_{yy}^T - 2\mathbf{Y}^T \mathbf{Y}, \quad (33c)$$

where the square matrices  $\mathbf{R} = [r_{ij}] \in \mathbb{R}^{N \times N}$ ,  $\dot{\mathbf{R}} = [\dot{r}_{ij}] \in \mathbb{R}^{N \times N}$  and  $\ddot{\mathbf{R}} = [\ddot{r}_{ij}] \in \mathbb{R}^{N \times N}$  contain the initial pairwise ranges, range rates and rates of range rates, respectively.

It is evident from (33) that without a priori knowledge of a few known PV, estimating the PVs of the network is an ill-posed problem and hence, we look to find solutions for the relative PV. Applying the centering matrix  $\mathbf{P} = \mathbf{I}_N - N^{-1} \mathbf{1}_N \mathbf{1}_N^T \in \mathbb{R}^{N \times N}$  on (33), and defining

$$\mathbf{B}_{xx} \triangleq -0.5\mathbf{P}\mathbf{R}^{\circ 2}\mathbf{P}, \quad (34a)$$

$$\mathbf{B}_{xy} \triangleq -\mathbf{P}(\mathbf{R} \circ \dot{\mathbf{R}})\mathbf{P}, \quad (34b)$$

$$\mathbf{B}_{yy} \triangleq -0.5\mathbf{P}(\mathbf{R} \circ \ddot{\mathbf{R}} + \dot{\mathbf{R}}^{\circ 2})\mathbf{P}, \quad (34c)$$

we have

$$\mathbf{B}_{xx} = \mathbf{P}\mathbf{X}^T \mathbf{X}\mathbf{P}, \quad (35a)$$

$$\mathbf{B}_{xy} = \mathbf{P}(\mathbf{X}^T \mathbf{Y} + \mathbf{Y}^T \mathbf{X})\mathbf{P}, \quad (35b)$$

$$\mathbf{B}_{yy} = \mathbf{P}\mathbf{Y}^T \mathbf{Y}\mathbf{P}. \quad (35c)$$

where we exploit the property  $\mathbf{P}\mathbf{1}_N = \mathbf{0}_N$ . Eqs. (35a) and (35c) can now be used to estimate the initial relative positions and relative velocities of the nodes, via MDS which will be addressed in Section 5. However, the MDS algorithm recovers  $\mathbf{X}$  and  $\mathbf{Y}$  only up to a rotation and translation. Therefore, prior to applying MDS we first define the relative PVs and subsequently present a relative framework of the absolute mobility model (30).

##### 4.3. Relative linear motion

We define the relative PV vectors as an affine transformation of the corresponding absolute PV  $(\mathbf{X}_k, \mathbf{Y})$  i.e.,

$$\tilde{\mathbf{X}}_k = \mathbf{H}_{x,k} \mathbf{X}_k + \mathbf{h}_{x,k} \mathbf{1}_N^T, \quad (36)$$

$$\mathbf{Y} = \mathbf{H}_y \mathbf{Y} + \mathbf{h}_y \mathbf{1}_N^T, \quad (37)$$

where  $\tilde{\mathbf{X}}_k$  is the relative position matrix of the nodes at  $t_k$  up to a rotation  $\mathbf{H}_{x,k} \in \mathbb{R}^{P \times P}$  and translation  $\mathbf{h}_{x,k} \in \mathbb{R}^{P \times 1}$ . Along similar lines, we define relative velocity as  $\mathbf{H}_y \mathbf{Y}$  and relative velocity up to a rotation as  $\mathbf{Y}$ , where  $\mathbf{H}_y \in \mathbb{R}^{P \times P}$  is an unknown rotation matrix. The relative velocity of the nodes  $\mathbf{H}_y \mathbf{Y}$  is relative to the group velocity of the network,

which is  $\mathbf{h}_y \in \mathbb{R}^{P \times 1}$ . Under a linear velocity assumption (29), the group velocity is the rate at which the translation vector varies with time i.e.,

$$\mathbf{h}_y = \Delta t_k^{-1}(\mathbf{h}_{x,k} - \mathbf{h}_{x,0}). \quad (38)$$

Furthermore, the rotation matrices  $\mathbf{H}_{x,k}$  and  $\mathbf{H}_y$  are orthogonal i.e.,

$$\mathbf{H}_{x,k}^T \mathbf{H}_{x,k} = \mathbf{H}_y^T \mathbf{H}_y = \mathbf{I}_p. \quad (39)$$

Now, substituting (36) and (37) in (30), and using the property (38) we have

$$\mathbf{H}_{x,k} \tilde{\mathbf{X}}_k = \mathbf{H}_{x,0} \mathbf{X} + \Delta t_k \mathbf{H}_y \mathbf{Y}, \quad (40)$$

where for the sake of notational simplicity, we use  $\mathbf{X} \triangleq \mathbf{X}_0$  to denote the relative position matrix at  $t_0$ .

Now observe that the translation vectors  $\mathbf{h}_{x,k}$  and  $\mathbf{h}_y$  are unidentifiable from observations (35). Subsequently, we shall also see in the following section that the solution to the relative PVs are independent of the translation vectors  $\mathbf{h}_x$  and  $\mathbf{h}_y$  and hence without loss of generality can be considered to be  $\mathbf{0}_p$  for notational simplicity. Secondly, in order to have a meaningful interpretation of the relative position at the  $k$ th time instant (40), we must choose a reference coordinate system e.g.,  $\mathbf{H}_{x,0} = \mathbf{I}$ . To this end, without loss of generality and for notational simplicity, we make the following assumptions:

$$\mathbf{H}_{x,0} = \mathbf{I}_p, \quad (41a)$$

$$\mathbf{h}_{x,0} = \mathbf{0}_p, \quad (41b)$$

$$\mathbf{h}_y = \mathbf{0}_p. \quad (41c)$$

Now defining  $\mathbf{X}_k \triangleq \mathbf{H}_{x,k} \tilde{\mathbf{X}}_k$  simplifies (40) to

$$\mathbf{X}_k = \mathbf{X} + \Delta t_k \mathbf{H}_y \mathbf{Y}, \quad (42)$$

where  $\mathbf{X}_k$  is the position of the nodes at the  $k$ th time instant up to a translation and  $r$ , under the assumption (41). More significantly, observe that the relative position at each  $k$ th time instant is only dependent on the relative PV and  $\mathbf{H}_y$ . Hence in the following sections, we estimate  $\mathbf{X}$ ,  $\mathbf{Y}$  and  $\mathbf{H}_y$  using the range parameters  $(\mathbf{R}, \hat{\mathbf{R}}, \hat{\mathbf{R}})$ , which was previously defined in (35) and estimated in Section 3.

#### 4.4. Relative kinematic matrices

Substituting the expression for absolute PV from (36) and (37) in (35), we have

$$\mathbf{B}_{xx} = \mathbf{P} \mathbf{X}^T \mathbf{X} \mathbf{P} = \mathbf{P} \mathbf{X}^T \mathbf{H}_{x,0}^T \mathbf{H}_{x,0} \mathbf{X} \mathbf{P} = \mathbf{X}^T \mathbf{X}, \quad (43a)$$

$$\begin{aligned} \mathbf{B}_{xy} &= \mathbf{P}(\mathbf{X}^T \mathbf{Y} + \mathbf{Y}^T \mathbf{X}) \mathbf{P} \\ &= \mathbf{P}(\mathbf{X}^T \mathbf{H}_{x,0}^T \mathbf{H}_y \mathbf{Y} + \mathbf{Y}^T \mathbf{H}_y^T \mathbf{H}_{x,0} \mathbf{X}) \mathbf{P} \\ &= \mathbf{X}^T \mathbf{H}_y \mathbf{Y} + \mathbf{Y}^T \mathbf{H}_y^T \mathbf{X}, \end{aligned} \quad (43b)$$

$$\mathbf{B}_{yy} = \mathbf{P} \mathbf{Y}^T \mathbf{Y} \mathbf{P} = \mathbf{P} \mathbf{Y}^T \mathbf{H}_y^T \mathbf{H}_y \mathbf{Y} \mathbf{P} = \mathbf{Y}^T \mathbf{Y}, \quad (43c)$$

where we use the property (39) in (43a) and (43c), and the assumption (41a) in (43b).  $\mathbf{B}_{xx}$  and  $\mathbf{B}_{yy}$  are Gramian matrices of the relative PVs and the expression for  $\mathbf{B}_{xy}$  is the Lyapunov-like linear matrix equation [17]. It is worth noting that the relative kinematic equations  $\mathbf{B}_{xx}$ ,  $\mathbf{B}_{xy}$ , and  $\mathbf{B}_{yy}$  are dependent only on the relative PVs and the unique

rotation matrix  $\mathbf{H}_y$  at time  $t_0$ . For an alternative derivation of the relative kinematic matrices, refer to Appendix B.

Given an estimate of the range matrices, i.e.,  $\hat{\mathbf{R}}, \hat{\mathbf{R}}$ , and  $\hat{\mathbf{R}}$ , either using (23) or alternative methods, an estimate of the relative kinematic matrices, i.e.,  $\hat{\mathbf{B}}_{xx}$ ,  $\hat{\mathbf{B}}_{xy}$ , and  $\hat{\mathbf{B}}_{yy}$  can be readily obtained using (34). Following this, we aim to estimate the relative position using (43a), the relative velocity using (43c) and the unknown velocity rotation matrix  $\mathbf{H}_y$  using (43b).

## 5. Estimation algorithms for $\mathbf{X}$ , $\mathbf{Y}$ , $\mathbf{H}_y$

### 5.1. Relative PVs ( $\mathbf{X}$ , $\mathbf{Y}$ )

An estimate of the relative PV can be directly obtained by the spectral decomposition of the matrices  $\mathbf{B}_{xx}$  and  $\mathbf{B}_{yy}$ . Let

$$\hat{\mathbf{B}}_{xx} = \mathbf{U}_x \mathbf{\Lambda}_x \mathbf{U}_x^T, \quad (44)$$

$$\hat{\mathbf{B}}_{yy} = \mathbf{U}_y \mathbf{\Lambda}_y \mathbf{U}_y^T, \quad (45)$$

where  $\mathbf{U}_x, \mathbf{U}_y \in \mathbb{R}^{N \times N}$  contain the eigenvectors and the diagonal matrices  $\mathbf{\Lambda}_x, \mathbf{\Lambda}_y \in \mathbb{R}^{N \times N}$  contain the increasingly ordered eigenvalues of the matrices  $\hat{\mathbf{B}}_{xx}, \hat{\mathbf{B}}_{yy}$  respectively. Then, for a  $P$ -dimensional setup, an estimate of the relative positions  $\mathbf{X}$  and relative velocities  $\mathbf{Y}$  of the nodes up to a rotation is then

$$\hat{\mathbf{X}} = \mathbf{\Lambda}_x^{1/2} \mathbf{U}_x^T, \quad (46)$$

$$\hat{\mathbf{Y}} = \mathbf{\Lambda}_y^{1/2} \mathbf{U}_y^T, \quad (47)$$

where  $\mathbf{\Lambda}_x, \mathbf{\Lambda}_y \in \mathbb{R}^{P \times P}$  contain the first  $P$  nonzero eigenvalues and  $\mathbf{U}_x, \mathbf{U}_y \in \mathbb{R}^{N \times P}$  contain the corresponding eigenvectors.

Relative positioning (46) from pairwise distance measurements using MDS is a well known technique [3]. However, our contribution is the definition and estimation of relative velocities, i.e., (37) and (47) respectively.

### 5.2. Rotation matrix $\mathbf{H}_y$

The estimate of the relative velocity  $\mathbf{Y}$  up to an arbitrary rotation gives no information on the direction of the nodes in an anchorless scenario. Hence, it is important to estimate the relative velocities w.r.t. the orientation of the initial positions i.e.,  $\mathbf{H}_y$ . Substituting the estimates of  $\mathbf{B}_{xy}$ ,  $\mathbf{X}$ , and  $\mathbf{Y}$  from (34b), (46) and (47) respectively in (43b), we have

$$\hat{\mathbf{B}}_{xy} = \hat{\mathbf{X}}^T \mathbf{H}_y \hat{\mathbf{Y}} + \hat{\mathbf{Y}}^T \mathbf{H}_y^T \hat{\mathbf{X}}, \quad (48)$$

where  $\mathbf{H}_y$  is the unknown rotation matrix. Now, vectorizing (48) and rearranging the terms, we have

$$\begin{aligned} \hat{\mathbf{b}}_{xy} &= (\hat{\mathbf{Y}}^T \otimes \hat{\mathbf{X}}^T) \text{vec}(\mathbf{H}_y) + (\hat{\mathbf{X}}^T \otimes \hat{\mathbf{Y}}^T) \text{vec}(\mathbf{H}_y^T) \\ &= (\mathbf{I}_{N^2} + \mathbf{J})(\hat{\mathbf{Y}}^T \otimes \hat{\mathbf{X}}^T) \text{vec}(\mathbf{H}_y) \\ &= \hat{\mathbf{G}} \text{vec}(\mathbf{H}_y), \end{aligned} \quad (49)$$

where  $\hat{\mathbf{b}}_{xy} = \text{vec}(\hat{\mathbf{B}}_{xy})$  is a vector of the known measurement matrix  $\hat{\mathbf{B}}_{xy}$  from (35b) and  $\mathbf{J} \in \mathbb{R}^{N^2 \times N^2}$  is an orthogonal permutation matrix such that  $\mathbf{J} \text{vec}(\mathbf{H}_y) = \text{vec}(\mathbf{H}_y^T)$ . Let  $\hat{\mathbf{H}}_y$  be

an estimate of  $\mathbf{H}_y$ , the unknown rotation can be obtained by minimizing the cost function:

$$\hat{\mathbf{H}}_y = \arg \min_{\mathbf{H}_y} \|\hat{\mathbf{G}}\text{vec}(\mathbf{H}_y) - \hat{\mathbf{b}}_{xy}\|^2. \quad (50)$$

Now, let the singular value decomposition of the augmented matrix  $\mathbf{S} = [\hat{\mathbf{G}} \ \hat{\mathbf{b}}_{xy}]$  be

$$\mathbf{S} = [\mathbf{U}_{s1} \ \mathbf{U}_{s2}] \begin{bmatrix} \Lambda_{s1} & \\ & \Lambda_{s2} \end{bmatrix} \begin{bmatrix} \mathbf{V}_{s11} \ \mathbf{V}_{s12} \\ \mathbf{V}_{s21} \ \mathbf{V}_{s22} \end{bmatrix}^T, \quad (51)$$

then the total least squares solution for minimizing the cost function (50) is

$$\text{vec}(\hat{\mathbf{H}}_y) = -\mathbf{V}_{s12} \mathbf{V}_{s22}^{-1}, \quad (52)$$

which has a feasible solution for  $N \geq P$ . The proposed solution does not exploit the orthogonality property of the unknown rotation matrix  $\mathbf{H}_y$ . Hence, more optimal solutions are feasible by solving the constrained least squares problem on the Stiefel manifold [18]:

$$\arg \min_{\mathbf{H}_y} \|\hat{\mathbf{G}}\text{vec}(\mathbf{H}_y) - \hat{\mathbf{b}}_{xy}\|^2 \quad \text{s.t.} \ \mathbf{H}_y^T \mathbf{H}_y = \mathbf{I}_P, \quad (53)$$

which is beyond the scope of this paper and will be addressed in a follow-up work.

### 5.3. Cramér Rao bounds

The Cramér Rao Bounds (CRB) for relative positioning were studied in [19,20], however the Fisher Information Matrix (FIM) for a general  $P$ -dimensional anchorless network was not investigated, which we present here. Furthermore, we also derive a lower bound for the proposed relative velocity estimator.

The CRB for any unbiased estimate of the unknown relative PVs

$$\boldsymbol{\phi}_x \triangleq \text{vec}(\mathbf{X}) = [\mathbf{x}_1^T, \mathbf{x}_2^T, \dots, \mathbf{x}_N^T]^T \in \mathbb{R}^{NP \times 1}, \quad (54)$$

$$\boldsymbol{\phi}_y \triangleq \text{vec}(\mathbf{Y}) = [\mathbf{y}_1^T, \mathbf{y}_2^T, \dots, \mathbf{y}_N^T]^T \in \mathbb{R}^{NP \times 1}, \quad (55)$$

are given by the inverse of the respective FIM i.e.,

$$\text{tr}(\mathbb{E}\{(\hat{\boldsymbol{\phi}}_x - \boldsymbol{\phi}_x)(\hat{\boldsymbol{\phi}}_x - \boldsymbol{\phi}_x)^T\}) \triangleq \text{tr}(\boldsymbol{\Sigma}_x) \geq \text{tr}(\mathbf{F}_x^{\dagger}), \quad (56)$$

$$\text{tr}(\mathbb{E}\{(\hat{\boldsymbol{\phi}}_y - \boldsymbol{\phi}_y)(\hat{\boldsymbol{\phi}}_y - \boldsymbol{\phi}_y)^T\}) \triangleq \text{tr}(\boldsymbol{\Sigma}_y) \geq \text{tr}(\mathbf{F}_y^{\dagger}), \quad (57)$$

where  $\{\hat{\boldsymbol{\phi}}_x, \hat{\boldsymbol{\phi}}_y\}$  are estimates of the unknown relative PVs  $\{\boldsymbol{\phi}_x, \boldsymbol{\phi}_y\}$  and  $\{\boldsymbol{\Sigma}_x, \boldsymbol{\Sigma}_y\}$  are the corresponding lowest achievable covariances. The FIMs for relative PVs are given by  $\mathbf{F}_x$  (see Appendix C) and  $\mathbf{F}_y$  (see Appendix D) respectively.

The derived FIMs are singular in the absence of anchor information. More specifically, for a 2-dimensional network the FIM for relative positions and relative velocities are rank deficient by 3. Since the FIM are not invertible, we use the pseudoinverse of the FIM as a lower bound to verify the optimality of the proposed estimators. Such scenarios arise in reference-free clock estimation [12], anchor-deficient localization [20], blind channel estimation [21] and array calibration [22] to name a few, where the inverse of the rank-deficient FIM is replaced by the pseudoinverse. This approach can be reasoned by investigating the CRB for a constrained framework.

When the FIM is singular, a set of linearly independent constraints, say  $\mathbf{C}$ , is required on the unknown parameters to

obtain the CRB. Let  $\mathbf{U}_c$  be an orthonormal basis for the null space of this constraint matrix  $\mathbf{C}$ , then the CRB for the constrained scenario is given by  $\text{tr}(\mathbf{U}_c(\mathbf{U}_c^T \mathbf{F} \mathbf{U}_c)^{-1} \mathbf{U}_c^T)$  [23]. Now, let  $\mathbf{F} \triangleq \mathbf{U}_f \Lambda_f \mathbf{U}_f^T$  be the eigenvalue decomposition of the singular FIM. Then, the constrained CRB is lowest when the  $\mathbf{U}_c$  spans the range of  $\mathbf{F}$  [21], which simplifies the CRB to  $\text{tr}(\Lambda_f^{\dagger})$ , where  $\Lambda_f^{\dagger}$  is obtained by taking the reciprocal of each non-zero element along the diagonal and leaving the zeros in place. Observe that the pseudoinverse of the singular FIM yields exactly the same expression i.e.,  $\text{tr}((\mathbf{U}_f \Lambda_f \mathbf{U}_f^T)^{\dagger}) = \text{tr}(\Lambda_f^{\dagger})$ . Thus, among the set of all feasible linearly independent constraints, the pseudo-inverse of the unconstrained FIM yields the lowest value for the total variance on all estimated parameters. There exists no unbiased estimator which achieves this bound without a priori knowledge or additional constraints on the system, and hence the bounds (56) and (57) are termed *oracle-bounds*.

## 6. Relative positions over time

We now briefly summarize the steps to find the relative position at discrete time instances using the time stamp measurements discussed in Section 2.

### 6.1. Linearized MDS (LMDS)

Given the noisy time stamps  $\hat{T}_{ij,k} = T_{ij,k} + q_{i,k}$ ,  $\forall (i,j)$  node pairs in the network and  $\forall 1 \leq k \leq K$  time instances, the relative position of the nodes at the  $k$ th time instance can be estimated as follows:

1. Estimate the range derivatives  $\hat{\mathbf{R}}, \hat{\mathbf{R}}^{\dagger}$ , and  $\hat{\mathbf{R}}^{\dagger}$ 
  - (a) using Dynamic Ranging (23) and/or
  - (b) via Doppler measurements and/or by other means.
 Using these range derivatives, construct the relative
2. kinematic matrices  $\hat{\mathbf{B}}_{xx}, \hat{\mathbf{B}}_{xy}$ , and  $\hat{\mathbf{B}}_{yy}$  (34a).
3. Obtain an estimate of the relative position  $\hat{\mathbf{X}}$ , relative velocity  $\hat{\mathbf{Y}}$  and rotation matrix  $\hat{\mathbf{H}}_y$  from (36), (37) and (52) respectively.
4. Defining  $\Delta \hat{\mathbf{T}}_k = \hat{T}_{ij,k} - \hat{T}_{ij,0}$  and using (42), the relative position at the  $k$ th time instant is

$$\hat{\mathbf{X}}_{k,lmads} = \hat{\mathbf{X}} + \Delta \hat{\mathbf{T}}_k \hat{\mathbf{H}}_y \hat{\mathbf{Y}}. \quad (58)$$

### 6.2. Connected MDS (CMDS)

Alternatively, the relative positions of the nodes can also be estimated using MDS at each time instant. Let  $\mathbf{D}_k \triangleq c[\tau_{ij,k}] \in \mathbb{R}^{N \times N}$  be the EDM at each discrete time instant  $k$  where  $\tau_{ij,k} = E_{ij,k}(T_{ij,k} - T_{ji,k})$  (8). Furthermore, let  $\hat{\mathbf{D}}_k \triangleq c[\tau_{ij,k} + q_{ij,k}]$  be the corresponding noisy distance estimate where  $q_{ij,k}$  is the noise plaguing the measurements as shown in (12). Let  $-0.5\mathbf{P}(\hat{\mathbf{D}}_k^{\odot 2})\mathbf{P} = \bar{\mathbf{U}}_k \bar{\Lambda}_k \bar{\mathbf{U}}_k^T$  be an eigenvalue decomposition, then the solution to the relative position is

$$\hat{\mathbf{X}}_{k,cmds} = \bar{\Lambda}_k^{-1/2} \bar{\mathbf{U}}_k^T \quad (59)$$

**Table 1**  
Computational complexity of proposed estimators.

Algorithm	Dynamic ranging	MDS	Rotation matrix	FLOPS
CMDS	–	$K$	$K$	$K(12N^3 + 4NP^4 + 8P^6)$
LMDS	–	2	1	$24N^3 + 4NP^2 + 8P^3$
LMDS-dynamic ranging	1	2	1	$2KN^2L^2 + 24N^3 + 4NP^2 + 8P^3$

where  $\overline{\mathbf{A}}_k \in \mathbb{R}^{P \times P}$  contain the first  $P$  nonzero eigenvalues and  $\overline{\mathbf{U}}_k \in \mathbb{R}^{N \times P}$  the corresponding eigenvectors.

The relative position estimate using CMDS i.e.,  $\hat{\mathbf{X}}_{k,cm\text{ds}}$  is up to an arbitrary rotation and translation, unlike  $\mathbf{X}_{k,lm\text{ds}}$  which yields the relative position of the nodes up to a translation alone. Hence to align all the relative position estimates (59), a unique rotation matrix at each time instant  $k$  must be estimated. Under constant velocity assumption, note that

$$\mathbf{X}_{k-1} - 2\mathbf{X}_k + \mathbf{X}_{k+1} = \mathbf{0}_P, \quad (60)$$

and using (36) and multiplying by  $\mathbf{H}_k^T$ , we have

$$\mathbf{H}_k^T \mathbf{H}_{k-1} \mathbf{X}_{k-1} - 2\mathbf{X}_k + \mathbf{H}_k^T \mathbf{H}_{k+1} \mathbf{X}_{k+1} = \mathbf{0}_{P,N}. \quad (61)$$

Now, substituting the relative position estimates from (59), we have

$$\underbrace{\begin{bmatrix} \hat{\mathbf{X}}_{k-1,cm\text{ds}}^T & \hat{\mathbf{X}}_{k+1,cm\text{ds}}^T \end{bmatrix}}_{\hat{\mathbf{A}}_k} \underbrace{\begin{bmatrix} \mathbf{H}_k^T \mathbf{H}_{k-1} \\ \mathbf{H}_k^T \mathbf{H}_{k+1} \end{bmatrix}}_{\mathbf{\Theta}_k} = 2\hat{\mathbf{X}}_{k,cm\text{ds}}^T, \quad (62)$$

where  $\mathbf{\Theta}_k$  containing the unknown rotation matrices can be estimated by minimizing the  $l_2$  norm:

$$\hat{\mathbf{\Theta}}_k = \arg \min_{\mathbf{\Theta}_k} \|\hat{\mathbf{A}}_k \mathbf{\Theta}_k - 2\hat{\mathbf{X}}_{k,cm\text{ds}}^T\|^2, \quad (63)$$

which similar to (50) has a solution for  $N \geq P$ . We name the estimation of relative positions (59) and the subsequent rotation matrices (63) under constant velocity assumption as Connected MDS (CMDS).

### 6.3. Computational complexity

The computational complexity of the proposed estimators is listed in Table 1. We evaluate the computation costs based on Floating point OperationS (FLOPS), ignoring the negligibly less complex additions and subtractions. The columns indicate the algorithms, the number of executions for various methods and the total number of FLOPS for each algorithm. To implement Dynamic Ranging i.e., least squares estimator, we assume the Gram–Schmidt method. In case of MDS and Rotation matrix estimation we use the Golub–Reinsch based Singularvalue decomposition [24]. Observe that, in contrast to the CMDS which estimates the relative position and corresponding rotation matrices for all  $K$  time instances, the proposed LMDS estimator estimates only the relative position, relative velocity and a single rotation matrix. Furthermore, the CMDS estimates 2 rotation matrices at each time instant (63) and hence has a factor  $P^2$  more complexity in rotation matrix estimation. Overall, the LMDS shows clear advantage, as it reduces the use of the expensive Eigenvalue decomposition

for MDS and total least squares for rotation matrix estimation, in comparison to the CMDS algorithm.

## 7. Simulations

Simulations are conducted to evaluate the performance of the proposed solutions. We consider a cluster of  $N=5$  nodes in  $P=2$  dimensions, whose coordinates  $\mathbf{X}$  and velocities  $\mathbf{Y}$  are arbitrarily chosen as

$$\mathbf{X} = \begin{bmatrix} -629 & 311 & 123 & -503 & 297 \\ -812 & 929 & 237 & 490 & -662 \end{bmatrix} \text{m},$$

$$\mathbf{Y} = \begin{bmatrix} -5 & 5 & 4 & -5 & -2 \\ -8 & -9 & 2 & -5 & 5 \end{bmatrix} \text{m/s}.$$

Without loss of generality, we assume that all nodes employ one-way communication, i.e.,  $\mathbf{e}_{ij} = \mathbf{1}_K, \forall i, j \leq N$ . Furthermore, all nodes communicate with each other within the time interval  $\Delta t = [T_{ij,1}, T_{ij,K}] = [-2.5, 2.5]$  s and the transmit time markers are chosen to be linearly spaced within this interval. We consider a classical pairwise communication scenario, where all the pairwise communications are independent of each other and thus  $\mathbf{\Sigma} = \sigma^2 \mathbf{I}_{NK}$ .

The metric used to evaluate the performance of the distances and range parameters is the Root Mean Square Error (RMSE), given by  $\text{RMSE}(\mathbf{z}) = \sqrt{N_{\text{exp}}^{-1} \sum_{n=1}^{N_{\text{exp}}} \|\hat{\mathbf{z}}(n) - \mathbf{z}\|^2}$ , where  $\hat{\mathbf{z}}(n)$  is the  $N$ th estimate of the unknown vector  $\mathbf{z}$  during  $N_{\text{exp}} = 1000$  Monte Carlo runs. To qualify these estimates, the square Root of the Cramér Rao Bound (RCRB) is plotted along with the respective RMSE. We also use the same metric for evaluating the rotation  $\text{vec}(\mathbf{H}_y)$ . In contrast to the range parameters, the relative PVs ( $\hat{\mathbf{X}}, \hat{\mathbf{Y}}$ ) and  $\mathbf{X}_k$  are known only up to an arbitrary rotation. Hence, we define the RMSE for these matrices as  $\text{RMSE}(\mathbf{Z}) = \sqrt{N_{\text{exp}}^{-1} \sum_{n=1}^{N_{\text{exp}}} \|\text{vec}(\mathbf{H}\hat{\mathbf{Z}}(n) - \mathbf{Z}\mathbf{P})\|^2}$ , where  $\mathbf{P}$  is the centering matrix and  $\mathbf{H}$  is the optimal Procrustes rotation, given the matrix  $\mathbf{Z}$  and the corresponding estimate  $\hat{\mathbf{Z}}(n)$  of the  $N$ th Monte Carlo run. See Appendix E. The RCRBs derived for the relative PVs (Section 5.3) are plotted along with the corresponding RMSEs.

### 7.1. Range parameters

The Dynamic Ranging algorithm (23) is implemented for  $L=4$ , where the number of communications  $K$  is varied from 10 to 1000. The noise on the propagation delays is  $\sigma=0.1$  m, which is typical in classical TWR [25] or in conventional anchored MDS-based velocity estimation using Doppler measurements [6]. Fig. 2(a) shows the RMSE of the first 3 range coefficients (which are relevant for

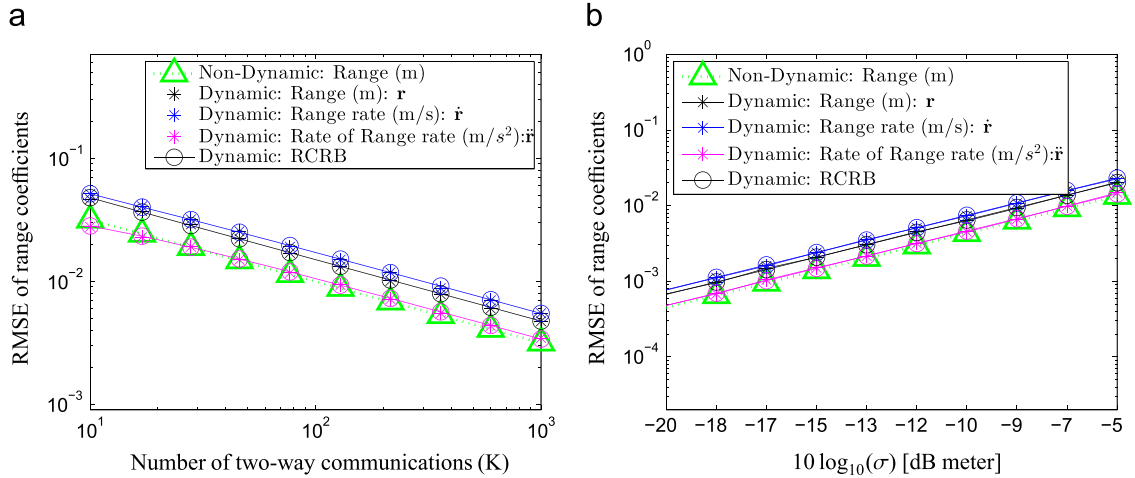


**Fig. 2.** RMSEs of range parameters (a) for varying number of communications ( $K$ ) between the nodes for  $\sigma = 0.1$  m and (b) for varying noise ( $\sigma$ ) on the time measurements with number of communication  $K = 500$ .

estimating the relative positions and velocities). A second experiment is carried out by varying  $\sigma$  in the range  $[-20, -5]$  dB m for a fixed number of communications  $K = 500$ . For the sake of comparison, we also plot the range estimate for the ‘non-dynamic’ scenario, where the nodes are immobile and the range between the nodes is fixed over the measurement period i.e., for  $\mathbf{Y} = \mathbf{0}_{2,N}$ . The RMSEs of the range coefficients obtained via the dynamic ranging algorithm (23) are plotted in Fig. 2(b). In both these experiments, the RMSEs of these range parameters achieve the corresponding RCRBs asymptotically for  $L = 4$ . Without loss of generality, we assume that the order of approximation is known, since iterative solutions such as iMGLS [12] can be employed to estimate  $L$ . For a detailed discussion on the effect of  $L$  on the distance estimation, particularly for an unsynchronized network, refer to our previous work [12].

### 7.2. Relative positions, velocities and rotation

The range parameters obtained via dynamic ranging are used to estimate the relative PV from (46) and (47). Fig. 3(a) shows the RMSEs of the PV plotted along with the respective RCRBs, for varying number of two-way communications  $K$  and Fig. 3(b) shows the RMSE plots for the relative PVs for varying signal-to-noise ratio. For the given experimental setup, the estimates are shown to perform reasonably well against the derived *oracle-bounds*. Furthermore, it is observed that the performance of the relative velocity is poorer in comparison to the relative positions. This is primarily because the measurement matrix for the relative velocity estimation  $\mathbf{B}_{yy}$  is dependent on  $\mathbf{R}$ ,  $\dot{\mathbf{R}}$ , and  $\ddot{\mathbf{R}}$ , whereas the relative position estimation relies only on the EDM  $\mathbf{R}$ . Hence, we observe that the magnitude of the noise covariance on the velocity model  $\Sigma_{yy}$  (D.5) is much larger than that of the position model  $\Sigma_{yx}$  (C.3). However, improved solutions can be expected if the Doppler measurements (such as radial velocity  $\dot{\mathbf{R}}$ ) are made available. The RMSEs of the relative rotation matrix  $\mathbf{H}_y$  estimate (52) are plotted in Fig. 4, where the relative PV estimates are used.

### 7.3. Relative position over time $t_k$

To illustrate the benefits of jointly estimating the relative PVs of the network, we simulate the proposed LMDS and CMDS algorithms. The relative PV and the rotation matrix estimates are used to realize the relative position of the nodes across time using LMDS (58). For the sake of comparison, the CMDS solution is also evaluated by estimating the relative positions using MDS (59) and the corresponding rotation matrix (63) at each time instant  $t_k$ . Fig. 5(a) shows the RMSE plots for  $\mathbf{X}_{k,\text{cmds}}$  and  $\mathbf{X}_{k,\text{lmds}}$  around the region of interest i.e.,  $t_0 = 0$  with Gaussian noise of  $\sigma = 0.1$  m and varying communication links  $K = [100, 300, 500]$ . Secondly, for a fixed  $K = 500$ , the signal-to-noise ratio is varied  $\sigma = [-3$  dB,  $-10$  dB,  $-20$  dB] and the LMDS is compared against CMDS in Fig. 5(b). The  $\mathbf{X}_{k,\text{cmds}}$  estimate steadily achieves a constant RMSE, which is expected since CMDS is independently applied at each  $k$ th time instant. On the contrary, the relative position estimation via dynamic ranging better this estimate around  $t_0$ , where the improvement of up to a factor  $\sqrt{K}$  is primarily due to averaging over  $K$  measurements. However, the error estimate of  $\mathbf{X}_{k,\text{lmds}}$  increases as we move away from  $t_0$ , which is typical of Taylor series approximation. Note that without loss of generality the range derivatives can be estimated in general for any  $t_0$  along the time interval. Hence, the relative PVs can be jointly estimated along the time-line, yielding improved solutions compared to CMDS at any given time instant.

## 8. Conclusions

We proposed a novel relative localization framework for an *anchorless network of mobile nodes*, given only the time-varying pairwise distances. Given the inter-nodal distances over time, the dynamic ranging algorithm employs a classical Taylor series based approximation, which extracts pairwise distance derivatives at any given time instant efficiently. Under linear velocity assumption, these derivatives are used to jointly estimate the initial relative PVs and a unique

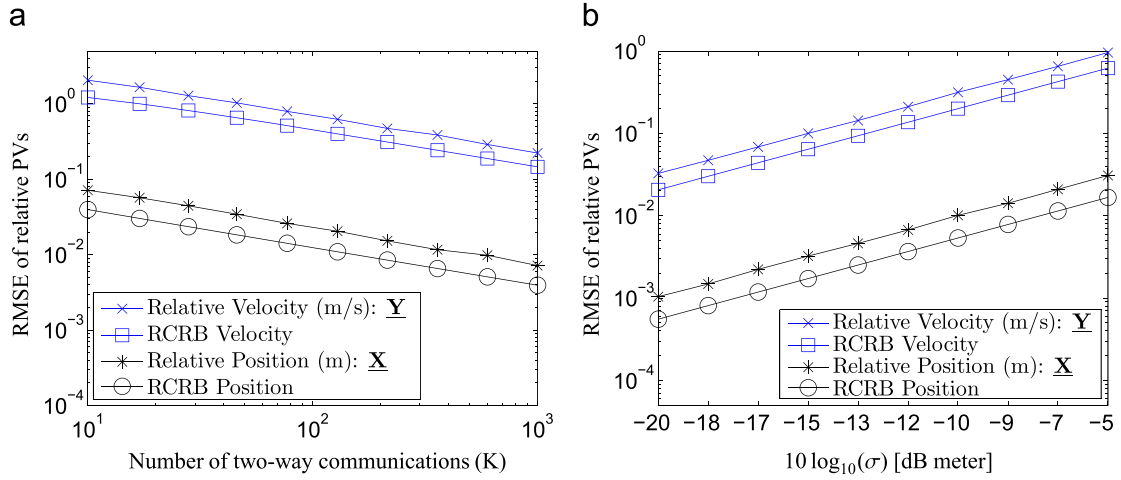


**Fig. 3.** RMSEs of relative positions and velocities (a) for varying number of communications ( $K$ ) between the nodes for  $\sigma = 0.1$  m and (b) for varying noise ( $\sigma$ ) on the time measurements with number of communication  $K=500$ .

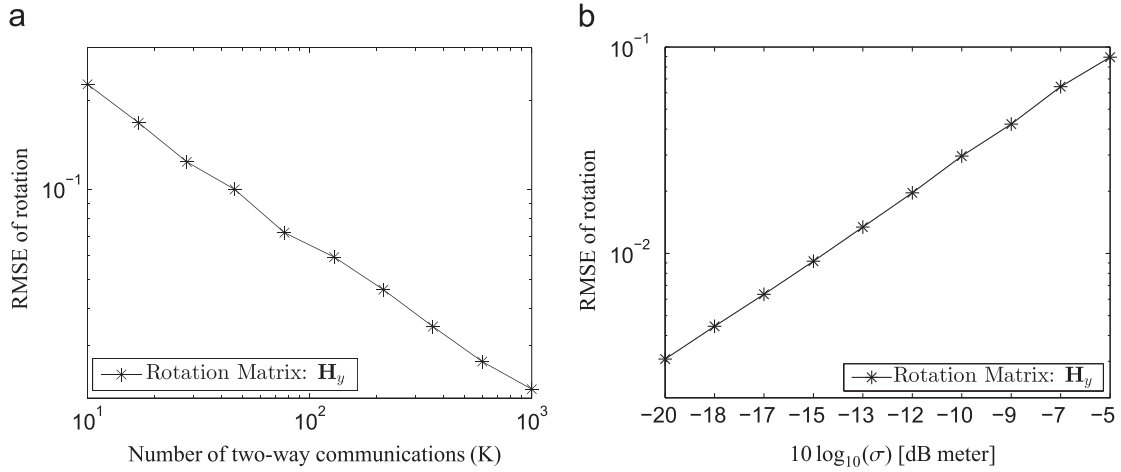


**Fig. 4.** RMSE of rotation matrix (a) for varying number of communications ( $K$ ) between the nodes for  $\sigma = 0.1$  m and (b) for varying noise ( $\sigma$ ) on the time measurements with number of communication  $K=500$ .

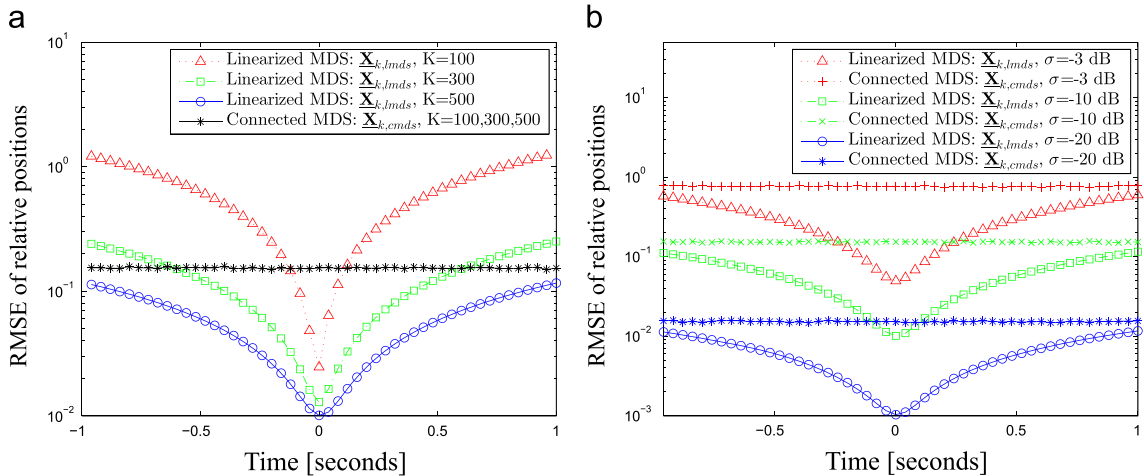


**Fig. 5.** RMSE of relative positions over time  $t_k$  around  $t_0 = 0$  (a) for  $K = [100, 300, 500]$  communication links with noise on time measurements  $\sigma = 0.1$  m and (b) for varying signal-to-noise ratio  $\sigma = [-3, -10, -20]$  dB with fixed  $K=500$ .

rotation matrix. We propose the LMDS algorithm, which combines the relative PVs and the rotation matrix to beget the relative motion of the nodes at discrete time instances. The LMDS can be considered as an extension of the well-known MDS. In addition, we also propose the CMDS where the relative node positions and the corresponding rotation matrices are estimated at each time instant. The Cramér Rao bounds are also derived for the range parameters, and the relative PV and simulations are conducted to verify the performance of the proposed estimators. While the CMDS shows consistent performance over time, the LMDS is computationally cost effective and shows up to a factor  $\sqrt{(K)}$  improvement around the region of interest. Furthermore, the LMDS permits the usage of Doppler measurements if available. The presented solutions are suited for autonomous networks with minimal a priori knowledge, where the positions and velocities need to be estimated at *cold start*. In practice, over longer durations, the estimated parameters can be readily extended to both relative and absolute tracking, which will be addressed in a follow-up work.

### Appendix A. Distance non-linearity

Consider an arbitrary pair of nodes  $\{i, j\}$  with initial positions  $\{\mathbf{x}_i, \mathbf{x}_j\}$  at  $t = t_0$  and constant velocities  $\{\mathbf{y}_i, \mathbf{y}_j\}$ , then the pairwise distance at  $t = t_k$  is

$$\begin{aligned} d_{ij,k} &= \|(\mathbf{x}_i - \mathbf{x}_j) - (\mathbf{y}_i - \mathbf{y}_j)t_k\| \\ &= \sqrt{\mathbf{x}_{ij}^T \mathbf{x}_{ij} - \mathbf{y}_{ij}^T \mathbf{y}_{ij} t_k^2 - 2\mathbf{x}_{ij}^T \mathbf{y}_{ij} t_k}, \end{aligned} \quad (\text{A.1})$$

where  $\mathbf{x}_{ij} = \mathbf{x}_i - \mathbf{x}_j$  and  $\mathbf{y}_{ij} = \mathbf{y}_i - \mathbf{y}_j$ , which shows that the pairwise distance is non-linear in time.

Let  $\{\bar{\mathbf{x}}_i(t), \bar{\mathbf{x}}_j(t)\}$  be the time varying positions of the node pair and  $d_{ij}(t)$  be the corresponding pairwise distance at time  $t$ , then the range parameters are derived as follows. By definition, the pairwise range between the nodes is the Euclidean norm

$$r_{ij} \triangleq d_{ij}(t_0) = \|\mathbf{x}_i - \mathbf{x}_j\|, \quad (\text{A.2})$$

From (A.2), we compute the first-order range parameter as

$$\begin{aligned} \dot{r}_{ij} &= \frac{d}{dt} d_{ij}(t) \\ &= \frac{1}{2r_{ij}} \frac{d}{dt} \left( (\bar{\mathbf{x}}_i(t) - \bar{\mathbf{x}}_j(t))^T (\bar{\mathbf{x}}_i(t) - \bar{\mathbf{x}}_j(t)) \right) \\ &= \frac{1}{r_{ij}} \left( \mathbf{y}_i^T \mathbf{x}_i + \mathbf{y}_j^T \mathbf{x}_j - \mathbf{y}_i^T \mathbf{x}_j - \mathbf{y}_j^T \mathbf{x}_i \right) \\ &= r_{ij}^{-1} (\mathbf{y}_i - \mathbf{y}_j)^T (\mathbf{x}_i - \mathbf{x}_j). \end{aligned} \quad (\text{A.3})$$

Similarly, under the assumption of constant velocities, the second-order range parameter using (A.2) is

$$\begin{aligned} \ddot{r}_{ij} &= \frac{d^2}{dt^2} d_{ij}(t) \\ &= -r_{ij}^{-2} \dot{r}_{ij} \left( (\mathbf{y}_i - \mathbf{y}_j)^T (\mathbf{x}_i - \mathbf{x}_j) \right) \\ &\quad + r_{ij}^{-1} \frac{d}{dt} \left( (\mathbf{y}_i - \mathbf{y}_j)^T (\bar{\mathbf{x}}_i(t) - \bar{\mathbf{x}}_j(t)) \right) \\ &= -r_{ij}^{-1} \dot{r}_{ij}^2 + r_{ij}^{-1} (\mathbf{y}_i - \mathbf{y}_j)^T (\mathbf{y}_i - \mathbf{y}_j) \\ &= r_{ij}^{-1} (\|\mathbf{y}_i - \mathbf{y}_j\|^2 - \dot{r}_{ij}^2). \end{aligned} \quad (\text{A.4})$$

The third-order derivative of the range parameter under linear motion (A.2) yields

$$\begin{aligned} \dddot{r}_{ij} &= \frac{d^3}{dt^3} d_{ij}(t) \\ &= -r_{ij}^{-2} \ddot{r}_{ij} \left( \|\mathbf{y}_i - \mathbf{y}_j\|^2 - \dot{r}_{ij}^2 \right) - r_{ij}^{-1} \frac{d^2}{dt^2} \left( \dot{d}_{ij}(t) \right) \\ &= -r_{ij}^{-1} \dot{r}_{ij} \ddot{r}_{ij} - 2r_{ij}^{-1} \dot{r}_{ij} \ddot{r}_{ij} \\ &= -3r_{ij}^{-1} \dot{r}_{ij} \ddot{r}_{ij}. \end{aligned} \quad (\text{A.5})$$

The higher-order range derivatives can be derived along similar lines.

### Appendix B. Alternative derivation for $\mathbf{B}_{xx}, \mathbf{B}_{xy}, \mathbf{B}_{yy}$

With an abuse of notation, let  $\mathbf{D}(t) \in \mathbb{R}^{N \times N}$  be the time-varying Euclidean Distance Matrix (EDM) for a network of  $N$  nodes in  $P$ -dimensional Euclidean space and let

$$\mathbf{B}(t) = -0.5\mathbf{P}\mathbf{D}(t) \odot^2 \mathbf{P}, \quad (\text{B.1})$$

where  $\mathbf{P} = \mathbf{I}_N - N^{-1} \mathbf{1}_N \mathbf{1}_N^T$  is the centering matrix. Then observe that at  $t = t_0$ ,

$$\mathbf{B}(t_0) \triangleq \mathbf{B}_{xx} = \underline{\mathbf{X}}^T \underline{\mathbf{X}}, \quad (\text{B.2})$$

and the subsequent first derivative is

$$\begin{aligned} \mathbf{B}_{xy} &\triangleq \frac{d\mathbf{B}(t)}{dt} \triangleq -\mathbf{P} \left( \mathbf{D}(t) \odot \dot{\mathbf{D}}(t) \right) \mathbf{P} \Big|_{t=t_0} \\ &= \underline{\mathbf{X}}^T \mathbf{H}_{xy} \underline{\mathbf{Y}} + \underline{\mathbf{Y}}^T \mathbf{H}_{xy}^T \underline{\mathbf{X}}. \end{aligned} \quad (\text{B.3})$$

A step further, differentiating again w.r.t.time and substituting  $t = t_0$  we have

$$\frac{d^2 \mathbf{B}(t)}{dt^2} \Big|_{t=t_0} \triangleq \mathbf{B}_{yy} \triangleq -0.5\mathbf{P} \left( \mathbf{R} \odot \ddot{\mathbf{R}} + \dot{\mathbf{R}} \odot^2 \right) \mathbf{P} = \underline{\mathbf{Y}}^T \underline{\mathbf{Y}}, \quad (\text{B.4})$$

where  $\dot{\mathbf{R}} = [\dot{r}_{ij}] \in \mathbb{R}^{N \times N}$  and  $\ddot{\mathbf{R}} = [\ddot{r}_{ij}] \in \mathbb{R}_+^{N \times N}$  which, perhaps not surprisingly, concur with the relations obtained in (43) and offer an alternative verification.

Secondly, unlike the time-varying distance function  $\mathbf{D}(t)$ , which is infinitely differentiable,  $\mathbf{B}(t)$  is a second-order function under the linear velocity assumption (29). Differentiating (B.4) yet again, we have

$$\frac{d^3 \mathbf{B}(t)}{dt^3} \Big|_{t=t_0} = -0.5\mathbf{P} \left( \mathbf{R} \odot \ddot{\mathbf{R}} + 3\dot{\mathbf{R}} \odot \ddot{\mathbf{R}} \right) \mathbf{P} = \mathbf{0}_{N,N}, \quad (\text{B.5})$$

where

$$\ddot{\mathbf{R}} \triangleq \frac{d^2 \mathbf{R}}{dt^2} = -3\mathbf{R}^{-1} \odot \dot{\mathbf{R}} \odot \ddot{\mathbf{R}}. \quad (\text{B.6})$$

### Appendix C. FIM of the relative positions ( $\underline{\mathbf{X}}$ )

The problem of estimating the unknown positions  $\underline{\phi}_x \triangleq \text{vec}(\underline{\mathbf{X}}) = [\underline{\mathbf{x}}_1^T, \underline{\mathbf{x}}_2^T, \dots, \underline{\mathbf{x}}_N^T]^T \in \mathbb{R}^{NP \times 1}$  from the distance measurements is formulated as

$$\mathbf{a}_x(\underline{\phi}_x) - \mathbf{d}_x = \boldsymbol{\eta}_x, \quad (\text{C.1})$$

where the vector  $\mathbf{d}_x = \{r_{ij}\} \forall i, j \leq N, i \neq j \in \mathbb{R}^{2\bar{N} \times 1}$  is the set of distances between  $N$  points, with  $\bar{N} = \binom{N}{2}$ . The distance vector is related to the positions by  $\mathbf{a}(\underline{\phi}_x) = [a_x(\underline{\mathbf{x}}_1, \underline{\mathbf{x}}_2),$

$a_x(\mathbf{x}_1, \mathbf{x}_3), \dots, a_x(\mathbf{x}_{N-1}, \mathbf{x}_N)]^T \in \mathbb{R}^{2N \times 1}$  where

$$\mathbf{a}_x(\mathbf{x}_i, \mathbf{x}_j) \triangleq (\mathbf{x}_i^T \mathbf{x}_j + \mathbf{x}_j^T \mathbf{x}_i - 2\mathbf{x}_i^T \mathbf{x}_j)^{1/2}. \quad (\text{C.2})$$

Furthermore, the noise plaguing the distance vector is

$$\boldsymbol{\eta}_x \sim \mathcal{N}(0, \boldsymbol{\Sigma}_{\eta_x}) \quad \text{where } \boldsymbol{\Sigma}_{\eta_x} = \text{bdiag}(\boldsymbol{\Sigma}_r, \boldsymbol{\Sigma}_r), \quad (\text{C.3})$$

and  $\boldsymbol{\Sigma}_r$  is given by (28). For the data model (C.1), the FIM  $\mathbf{F}_x \in \mathbb{R}^{NP \times NP}$  is

$$\mathbf{F}_x = \left[ \frac{\partial \mathbf{a}_x(\boldsymbol{\phi}_x)}{\partial \boldsymbol{\phi}_x^T} \right]^T \boldsymbol{\Sigma}_{\eta_x}^{-1} \left[ \frac{\partial \mathbf{a}_x(\boldsymbol{\phi}_x)}{\partial \boldsymbol{\phi}_x^T} \right]. \quad (\text{C.4})$$

where the Jacobian is of the form

$$\frac{\partial \mathbf{a}_x(\boldsymbol{\phi}_x)}{\partial \boldsymbol{\phi}_x^T} = \left[ \frac{\partial a_x(\boldsymbol{\phi}_x)}{\partial \mathbf{x}_1^T}, \frac{\partial a_x(\boldsymbol{\phi}_x)}{\partial \mathbf{x}_2^T}, \dots, \frac{\partial a_x(\boldsymbol{\phi}_x)}{\partial \mathbf{x}_N^T} \right]. \quad (\text{C.5})$$

The  $i$ th element of the Jacobian  $[\partial a_x(\boldsymbol{\phi}) / \partial \mathbf{x}_i^T]$  is given by

$$\left[ \frac{\partial a(\mathbf{x}_1, \mathbf{x}_2)}{\partial \mathbf{x}_i^T}, \frac{\partial a(\mathbf{x}_1, \mathbf{x}_3)}{\partial \mathbf{x}_i^T}, \dots, \frac{\partial a(\mathbf{x}_{N-1}, \mathbf{x}_N)}{\partial \mathbf{x}_i^T} \right],$$

where  $\forall 1 \leq j, k \leq N, j \neq k$ , we have

$$\frac{\partial a(\mathbf{x}_j, \mathbf{x}_k)}{\partial \mathbf{x}_i^T} = \begin{cases} r_{jk}^{-1}(\mathbf{x}_j - \mathbf{x}_k)^T & \text{if } i = j & (\text{a}) \\ -r_{jk}^{-1}(\mathbf{x}_j - \mathbf{x}_k)^T & \text{if } i = k & (\text{b}) \\ \mathbf{0}_p^T & \text{otherwise} & (\text{c}) \end{cases} \quad (\text{C.6})$$

#### Appendix D. FIM of the relative velocities ( $\mathbf{Y}$ )

The estimation of relative velocities  $\boldsymbol{\phi}_x \triangleq \text{vec}(\mathbf{Y}) = [\mathbf{y}_1^T, \mathbf{y}_2^T, \dots, \mathbf{y}_N^T]^T \in \mathbb{R}^{NP \times 1}$  is modeled as

$$\mathbf{a}_y(\boldsymbol{\phi}_y) - \mathbf{d}_y^{\odot 2} = \boldsymbol{\eta}_y, \quad (\text{D.1})$$

where  $\mathbf{a}(\boldsymbol{\phi}_y) = [a_y(\mathbf{y}_1, \mathbf{y}_2), a_y(\mathbf{y}_1, \mathbf{y}_3), \dots, a_y(\mathbf{y}_{N-1}, \mathbf{y}_N)]^T \in \mathbb{R}^{2N \times 1}$  and

$$\mathbf{a}_y(\mathbf{y}_i, \mathbf{y}_j) \triangleq \mathbf{y}_i^T \mathbf{y}_i + \mathbf{y}_j^T \mathbf{y}_j - 2\mathbf{y}_i^T \mathbf{y}_j. \quad (\text{D.2})$$

The distance squared vector  $\mathbf{d}_y^{\odot 2} = \{r_{ij}^2 \ddot{r}_{ij} + \dot{r}_{ij}^{\odot 2}\} \forall i, j \leq N, i \neq j \in \mathbb{R}^{2N \times 1}$ , where  $r_{ij}$ ,  $\dot{r}_{ij}$ , and  $\ddot{r}_{ij}$  are the corresponding range estimates. The noise  $\boldsymbol{\eta}_y = \{\eta_{y,ij}\}$  in the data model is

$$\begin{aligned} \eta_{y,ij} &= r_{ij} q_{r,ij} + \dot{r}_{ij} q_{\dot{r},ij} + 2\ddot{r}_{ij} q_{\ddot{r},ij} + q_{r,ij} q_{\dot{r},ij} + q_{\dot{r},ij} q_{\ddot{r},ij} \\ &\approx r_{ij} q_{r,ij} + \dot{r}_{ij} q_{\dot{r},ij} + 2\ddot{r}_{ij} q_{\ddot{r},ij}, \end{aligned} \quad (\text{D.3})$$

where  $q_{r,ij}$ ,  $q_{\dot{r},ij}$ , and  $q_{\ddot{r},ij}$  are the noise variable plaguing the range parameters  $r_{ij}$ ,  $\dot{r}_{ij}$ , and  $\ddot{r}_{ij}$  respectively. The covariance of the noise is subsequently defined as

$$\boldsymbol{\Sigma}_{\eta_y} = \mathbb{E}\{\boldsymbol{\eta}_y \boldsymbol{\eta}_y^T\} \approx \text{bdiag}(\boldsymbol{\Sigma}_{\eta_y}, \boldsymbol{\Sigma}_{\eta_y}), \quad (\text{D.4})$$

where

$$\boldsymbol{\Sigma}_{\eta_y} \approx \mathbf{R} \boldsymbol{\Sigma}_r \mathbf{R} + \dot{\mathbf{R}} \boldsymbol{\Sigma}_{\dot{r}} \dot{\mathbf{R}} + 4\ddot{\mathbf{R}} \boldsymbol{\Sigma}_{\ddot{r}} \ddot{\mathbf{R}} \quad (\text{D.5})$$

$\mathbf{R} = \text{diag}(\mathbf{r})$ ,  $\dot{\mathbf{R}} = \text{diag}(\dot{\mathbf{r}})$ , and  $\ddot{\mathbf{R}} = \text{diag}(\ddot{\mathbf{r}})$  are the range parameters and  $\boldsymbol{\Sigma}_r$ ,  $\boldsymbol{\Sigma}_{\dot{r}}$ , and  $\boldsymbol{\Sigma}_{\ddot{r}}$  are the corresponding covariance matrices (28). The FIM  $\mathbf{F}_y \in \mathbb{R}^{NP \times NP}$  is then

$$\mathbf{F}_y = \left[ \frac{\partial \mathbf{a}_y(\boldsymbol{\phi}_y)}{\partial \boldsymbol{\phi}_y^T} \right]^T \boldsymbol{\Sigma}_{\eta_y}^{-1} \left[ \frac{\partial \mathbf{a}_y(\boldsymbol{\phi}_y)}{\partial \boldsymbol{\phi}_y^T} \right], \quad (\text{D.6})$$

where the Jacobian is of the form

$$\frac{\partial \mathbf{a}_y(\boldsymbol{\phi}_y)}{\partial \boldsymbol{\phi}_y^T} = \left[ \frac{\partial a_y(\boldsymbol{\phi}_y)}{\partial \mathbf{y}_1^T}, \frac{\partial a_y(\boldsymbol{\phi}_y)}{\partial \mathbf{y}_2^T}, \dots, \frac{\partial a_y(\boldsymbol{\phi}_y)}{\partial \mathbf{y}_N^T} \right]. \quad (\text{D.7})$$

The  $i$ th element of the Jacobian  $[\partial a_y(\boldsymbol{\phi}) / \partial \mathbf{y}_i^T]$  is given by

$$\left[ \frac{\partial a(\mathbf{y}_1, \mathbf{y}_2)}{\partial \mathbf{y}_i^T}, \frac{\partial a(\mathbf{y}_1, \mathbf{y}_3)}{\partial \mathbf{y}_i^T}, \dots, \frac{\partial a(\mathbf{y}_{N-1}, \mathbf{y}_N)}{\partial \mathbf{y}_i^T} \right],$$

where  $\forall 1 \leq j, k \leq N, j \neq k$ , we have

$$\frac{\partial a(\mathbf{y}_j, \mathbf{y}_k)}{\partial \mathbf{y}_i^T} = \begin{cases} 2(\mathbf{y}_j - \mathbf{y}_k)^T & \text{if } i = j & (\text{a}) \\ -2(\mathbf{y}_j - \mathbf{y}_k)^T & \text{if } i = k & (\text{b}) \\ \mathbf{0}_p^T & \text{otherwise} & (\text{c}) \end{cases} \quad (\text{D.8})$$

#### Appendix E. Procrustes alignment

Let  $\mathbf{Z}, \mathbf{Z} \in \mathbb{R}^{P \times N}$  be matrices identical up to a rotation and let  $\mathbf{U}_z$  contain the eigenvectors of the matrix product  $\mathbf{Z}\mathbf{Z}^T$ , then there exists a rotation matrix  $\mathbf{H}$  which minimizes the following cost function:

$$\min_{\mathbf{H}} \|\mathbf{Z} - \mathbf{H}\mathbf{Z}\| \quad \text{s.t.} \quad \mathbf{H}^T \mathbf{H} = \mathbf{I}_p, \quad (\text{E.1})$$

and the corresponding optimal Procrustes rotation [26] is

$$\hat{\mathbf{H}} = \mathbf{U}_z \mathbf{U}_z^T. \quad (\text{E.2})$$

#### References

- [1] R.T. Rajan, G. Leus, A.-J. van der Veen, Relative velocity estimation using multidimensional scaling, in: 2013 IEEE 5th International Workshop on Computational Advances in Multi-Sensor Adaptive Processing (CAMSAP), 2013, pp. 125–128. doi:<http://dx.doi.org/10.1109/CAMSAP.2013.6714023>.
- [2] A. Sayed, A. Tarighat, N. Khajehnouri, Network-based wireless location: challenges faced in developing techniques for accurate wireless location information, IEEE Signal Process. Mag. 22 (4) (2005) 24–40. <http://dx.doi.org/10.1109/MSP.2005.1458275>.
- [3] I. Borg, P.J.F. Groenen, Modern Multidimensional Scaling: Theory and Applications (Springer Series in Statistics), 2nd Edition, Springer, New York, NY, 2005.
- [4] K. Cheung, H. So, A multidimensional scaling framework for mobile location using time-of-arrival measurements, IEEE Trans. Signal Process. 53 (2) (2005) 460–470.
- [5] R.T. Rajan, A.-J. van der Veen, Joint ranging and clock synchronization for a wireless network, in: 2011 4th IEEE International Workshop on Computational Advances in Multi-Sensor Adaptive Processing (CAMSAP), 2011, pp. 297–300. doi: <http://dx.doi.org/10.1109/CAMSAP.2011.6136008>.
- [6] H.-W. Wei, R. Peng, Q. Wan, Z.-X. Chen, S.-F. Ye, Multidimensional scaling analysis for passive moving target localization With TDOA and FDOA measurements, IEEE Trans. Signal Process. 58 (3) (2010) 1677–1688. <http://dx.doi.org/10.1109/TSP.2009.2037666>.
- [7] V. Chandrasekhar, W.K. Seah, Y.S. Choo, H.V. Ee, Localization in underwater sensor networks: survey and challenges, in: Proceedings of the 1st ACM International Workshop on Underwater Networks, ACM, New York, NY, 2006, pp. 33–40.
- [8] H. Liu, H. Darabi, P. Banerjee, J. Liu, Survey of wireless indoor positioning techniques and systems, IEEE Trans. Appl. Rev. Syst. Man Cybern. Part C 37 (6) (2007) 1067–1080.
- [9] A. Bürkle, F. Segor, M. Kollmann, Towards autonomous micro UAV swarms, J. Intell. Robot. Syst. 61 (1–4) (2011) 339–353.
- [10] R.T. Rajan, S. Engelen, M. Bantum, C. Verhoeven, Orbiting low frequency array for radio astronomy, in: IEEE Aerospace Conference, 2011, pp. 1–11. doi: <http://dx.doi.org/10.1109/AERO.2011.5747222>.

- [11] R.T. Rajan, A.-J. van der Veen, Joint non-linear ranging and affine synchronization basis for a network of mobile nodes, in: 21st European Signal Processing Conference (EUSPICO), 2013, pp. 1–5.
- [12] R.T. Rajan, A.-J. vanderVeen, Joint ranging and synchronization for an anchorless network of mobile nodes, *IEEE Trans. Signal Process.* 63 (8) (2015) 1925–1940, <http://dx.doi.org/10.1109/TSP.2015.2391076>.
- [13] A. Bertrand, M. Moonen, Consensus-based distributed total least squares estimation in ad hoc wireless sensor networks, *IEEE Trans. Signal Process.* 59 (5) (2011) 2320–2330.
- [14] S.M. Kay, *Fundamentals of Statistical Signal Processing: Estimation Theory*, Prentice-Hall, Inc., Upper Saddle River, NJ, USA, 1993.
- [15] Part 15.4: Wireless Medium Access Control (MAC) and Physical Layer (PHY) Specifications for Low-rate Wireless Personal Area Networks (WPANs), Technical Report, IEEE Working Group 802.15.4, 2007.
- [16] Y. Wang, X. Ma, G. Leus, Robust time-based localization for asynchronous networks, *IEEE Trans. Signal Process.* 59 (9) (2011) 4397–4410, <http://dx.doi.org/10.1109/TSP.2011.2159215>.
- [17] H. Braden, The equations  $A^T X \pm X^T A = B$ , *SIAM J. Matrix Anal. Appl.* 20 (2) (1998) 295–302.
- [18] T. Viklands, Algorithms for the weighted orthogonal Procrustes problem and other least squares problems (Ph.D. thesis), Umeå University, Umeå, Sweden, 2006.
- [19] J. Ash, R. Moses, On the relative and absolute positioning errors in self-localization systems, *IEEE Trans. Signal Process.* 56 (11) (2008) 5668–5679, <http://dx.doi.org/10.1109/TSP.2008.927072>.
- [20] C. Chang, A. Sahai, Cramér–Rao-type bounds for localization, *EURASIP J. Appl. Signal Process.* (2006) 1–14.
- [21] E. de Carvalho, J. Cioffi, D. Slock, Cramér–Rao bounds for blind multichannel estimation, in: *IEEE Global Telecommunications Conference*, vol. 2, 2000, pp. 1036–1040.
- [22] S. Wijnholds, A.J. van der Veen, Effects of parametric constraints on the CRLB in gain and phase estimation problems, *Signal Process. Lett. IEEE* 13 (10) (2006) 620–623, <http://dx.doi.org/10.1109/LSP.2006.875348>.
- [23] P. Stoica, B.C. Ng, On the Cramer–Rao bound under parametric constraints, *Signal Process. Lett. IEEE* 5 (7) (1998) 177–179. doi: <http://dx.doi.org/10.1109/97.700921>.
- [24] G.H. Golub, C.F. Van Loan, *Matrix Computations*, JHU Press, Baltimore, Maryland, 2012.
- [25] N. Patwari, A. Hero, M. Perkins, N. Correal, R. O’Dea, Relative location estimation in wireless sensor networks, *IEEE Trans. Signal Process.* 51 (8) (2003) 2137–2148, <http://dx.doi.org/10.1109/TSP.2003.814469>.
- [26] P. Schönemann, A generalized solution of the orthogonal Procrustes problem, *Psychometrika* 31 (1) (1966) 1–10, <http://dx.doi.org/10.1007/BF02289451>.